

Host–Guest Systems

Direct Measurement of Electron Transfer in Nanoscale Host–Guest Systems: Metallocenes in Carbon Nanotubes

Robert L. McSweeney,^[a] Thomas W. Chamberlain,^[b] Matteo Baldoni,^[a] Maria A. Lebedeva,^[a, c] E. Stephen Davies,^[a] Elena Besley,^[a] and Andrei N. Khlobystov^{*,[a, d]}

Abstract: Electron-transfer processes play a significant role in host–guest interactions and determine physicochemical phenomena emerging at the nanoscale that can be harnessed in electronic or optical devices, as well as biochemical and catalytic systems. A novel method for qualifying and quantifying the electronic doping of single walled carbon nanotubes (SWNTs) using electrochemistry has been developed that establishes a direct link between these experimental measurements and ab initio DFT calculations. Metallocenes such as cobaltocene and methylated ferrocene derivatives were encapsulated inside SWNTs (1.4 nm diameter) and cyclic voltammetry (CV) was performed on the resultant

host–guest systems. The electron transfer between the guest molecules and the host SWNTs is measured as a function of shift in the redox potential ($E_{1/2}$) of $\text{Co}^{\text{II}}/\text{Co}^{\text{I}}$, $\text{Co}^{\text{III}}/\text{Co}^{\text{II}}$ and $\text{Fe}^{\text{III}}/\text{Fe}^{\text{II}}$. Furthermore, the shift in $E_{1/2}$ is inversely proportional to the nanotube diameter. To quantify the amount of electron transfer from the guest molecules to the SWNTs, a novel method using coulometry was developed, allowing the mapping of the density of states and the Fermi level of the SWNTs. Correlated with theoretical calculations, coulometry provides an accurate indication of n/p-doping of the SWNTs.

Introduction

The confinement of individual molecules inside nanoscale containers is a powerful method that allows us to explore chemistry at the single-molecule level.^[1,2] As the dimensions of the host container approach the size of the encapsulated molecule, the effects of extreme spatial constraint result in changes in van der Waals interactions and electron transfer, leading to new dynamic behaviour and the emergence of physicochemical properties of the confined molecules unattainable in the bulk.^[3–6]

Single-walled carbon nanotubes (SWNTs) are an increasingly popular choice as molecular containers as not only do they possess nanoscale cavities in the range of 0.7–2.0 nm, commensurate with small and medium sized molecules, but they also boast exciting electronic properties. The unique electronic

structure^[7] of SWNTs and the ability to exhibit either metallic or semiconducting behaviour depending only on chirality^[8] while interacting effectively with electron donors^[5,9,10] and acceptors^[11] make nanotubes highly tuneable nanoscale containers with respect to electronic interactions with guest molecules.

Previous studies on the nature of interactions between nanotubes and guest molecules have included the application of UV/Vis^[5] and IR^[11] spectroscopies to probe the confined molecules. The use of spectroscopy can be challenging, owing to the absorption of radiation by the host nanotube, which may obscure many important subtle features of the nanotube–molecule interactions. Other techniques have been employed to analyse the nanotube and guest molecule oxidation state using separate probes such as photoemission spectroscopy and X-ray absorption.^[12] An interesting method was reported that utilised an electrode to elevate the potential of the nanotube, which in turn perturbs the electronic state of the guest molecules, which is measured using Raman spectroscopy. However, this approach is limited to guest molecules with strong Raman vibration modes.^[13] Overall, as SWNTs interact strongly and absorb a wide range of electromagnetic radiation (UV/Vis, IR, near-IR), the use of spectroscopy to probe guest molecules inside nanotubes can be ambiguous because the spectroscopic signal of molecules adsorbed on the nanotube surface overpowers the weak signals of encapsulated molecules due to shielding by SWNTs.

An alternative approach is to exploit the highly electrically conductive nature of SWNTs and fast heterogeneous electron transfer at nanotube tips and sidewalls,^[14,15] which enables effi-

[a] R. L. McSweeney, Dr. M. Baldoni, Dr. M. A. Lebedeva, Dr. E. S. Davies, Prof. Dr. E. Besley, Prof. Dr. A. N. Khlobystov
School of Chemistry, University of Nottingham
University Park, Nottingham NG7 2RD (UK)

[b] Dr. T. W. Chamberlain
Institute of Process Research & Development, School of Chemistry
University of Leeds, Woodhouse Lane, Leeds LS2 9JT (UK)

[c] Dr. M. A. Lebedeva
Department of Materials, Oxford University
Oxford OX1 3PH (UK)

[d] Prof. Dr. A. N. Khlobystov
National University of Science & Technology, MISIS
Moscow 119049 (Russia)

Supporting information and ORCID(s) from the author(s) for this article are available on the WWW under <http://dx.doi.org/10.1002/open.201402097>.

cient charge transfer between guest molecules and the nanotube, to probe the confined molecules. In particular, electrochemical measurements offer an ideal method for precise characterisation of host–guest interactions between molecules and nanotubes.^[16] Cyclic voltammetry has been utilised successfully to study confined molecules and to tune their functional properties, as demonstrated in metal-organic frameworks (MOFs),^[17,18] zeolites^[19] and molecular cages.^[20–22] However, poor electrical conductivity of these host-structures prohibits reliable pathways for charge transfer between the electrode and confined guest molecules. In contrast, charge transport through the nanotube onto confined guest molecules is uninhibited and very efficient making SWNTs the ideal host systems for studying redox phenomena at the nanoscale.

Herein, we report an electrochemical study of redox-active guest molecules confined within carbon nanotubes and demonstrate that encapsulation in SWNTs alters the oxidation state of guest molecules. We demonstrate that the amount of electron transfer between the nanotube and molecules is precisely determined by the energy of the guest molecule HOMO/SOMO and the diameter of the SWNT. The interactions between molecules and nanotubes result in profound changes in the effective bandgap of the SWNTs,^[23,24] which can be modulated by choosing guest molecules with the appropriate HOMO/SOMO and gauged accurately by using a new coulometric approach developed in this study.

Results and Discussion

As fullerene (C₆₀) was the first guest molecule inserted into carbon nanotubes, the nature and strength of the interactions between fullerene molecules and the internal cavity of a nanotube have been extensively investigated.^[25–27] The perfect geometrical match of truncated icosahedral fullerene cages and the tubular interior of nanotubes provide extremely effective van der Waals interactions that can be as high as 3 eV per molecule.^[25] In contrast, although metal complexes have been encapsulated in nanotubes for a wide variety of applications, including catalysis,^[28–30] spintronics,^[31] and sensors,^[32] very little has been reported about the nature of their interactions with the nanotube cavity. The electric charge, asymmetrical distribution of the electron density, and the irregular shape of metal complexes make this a difficult challenge. A new methodology based on electrochemical measurement is employed in this study to probe interactions between metallocenes and SWNTs and to harness the well-defined redox properties of these guest species to control the electronic properties of the host SWNTs.

During linear-sweep voltammogram (LSV) measurements a potential is applied to carbon nanotubes attached to a glassy carbon electrode (Figures 1 and 2), and the current between the nanotube and electrode is measured. The magnitude of the current varies significantly and reveals distinguishable charging/discharging processes for the SWNTs (average diameter of 1.4 nm; Figure 1 a, red curve). We assume SWNTs to be a quantum capacitance-dominated electrode, such that application of potential in this system causes the shift of the

Fermi level.^[36,37] Mapping the experimental measurements onto the calculated density of states (DoS) of metallic (10,10) and semiconducting (17,0) SWNTs representative for this sample (Figure 1 a, blue and green curves, respectively) helps to understand the observed voltammogram.^[38] Hodge et al. reported a similar observation and band gap.^[39] In general, the increase in current is associated with the increase in density of full or empty states of the SWNTs, which are depleted or populated with electrons as the applied potential becomes more positive or negative, respectively. For instance, increased current is observed at -0.30 V, 0.50 V and 1.10 V, which corresponds to the three major maxima in DoS of nanotubes.^[7,40] Similarly, in the region between 0.1 V and -0.28 V, very low current is observed in the LSV, which correlates with the low DoS of SWNTs available in this energy window. Thus the two axes representing the applied potential (Figure 1 a, red vertical axis) and the energy levels of SWNTs (Figure 1 a, black vertical axis) plotted inverse to one another ($\Delta G = -nFE$), can link the LSV measurements with theoretically calculated DoS.

Cyclic voltammetry measurements on free molecules allow us to measure the first potential required to remove an electron from the HOMO/SOMO of the molecule. However, as electronic interactions between the host and the guest in molecule@SWNT systems will result in electron transfer, the oxidation state of the confined guest molecule is changed with no externally applied potential. As a result of this electron transfer, the energy of the Fermi level of the nanotube shifts (Figure 1 b) so that, when electric potential is applied, electrons are removed from a higher (in the case of an electron donor guest molecule) or lower (in the case of an electron acceptor guest molecule) energy level of the global molecule@SWNT system. Overall, the encapsulation of redox-active species into nanotubes can result in hybrid nanostructures with complex electrochemical properties, dramatically different to the properties of the individual components, which may complicate experimental measurements. However, if the synergistic effects of host–guest interactions are understood, they can shed light onto fundamental aspects of electron transfer.

The electrochemistry of ferrocene [Fe(Cp)₂] is the most studied amongst organometallic complexes, so this molecule represents the best starting point for the investigation of host–guest interactions with SWNTs. Upon encapsulation in nanotubes (Figure 3) by a previously reported gas-phase method,^[41] the redox potential ($E_{1/2}$) of the Fe^{III}/Fe^{II} couple of [Fe(Cp)₂] is observed to shift by $+0.04$ V compared to the same measurement performed for [Fe(Cp)₂] in solution, outside nanotubes (Figure 4). Such a small but measurable shift of the Fe^{III}/Fe^{II} couple was previously observed in other nanocontainers with a positive charge,^[20–22,42] and can be attributed to a decrease in electron density on the iron centre of [Fe(Cp)₂] compared to the solution CV. The HOMO of [Fe(Cp)₂] is below the Fermi level of the pristine nanotubes, which means that theoretically no spontaneous electron transfer can occur (Figure 1 b). However, in practice, carbon nanotubes have defects decorated with oxygen-containing groups resulting in a lower energy Fermi level (i.e., some degree of p-doping),^[34,35] which allows for some electron transfer to occur from ferrocene to the top

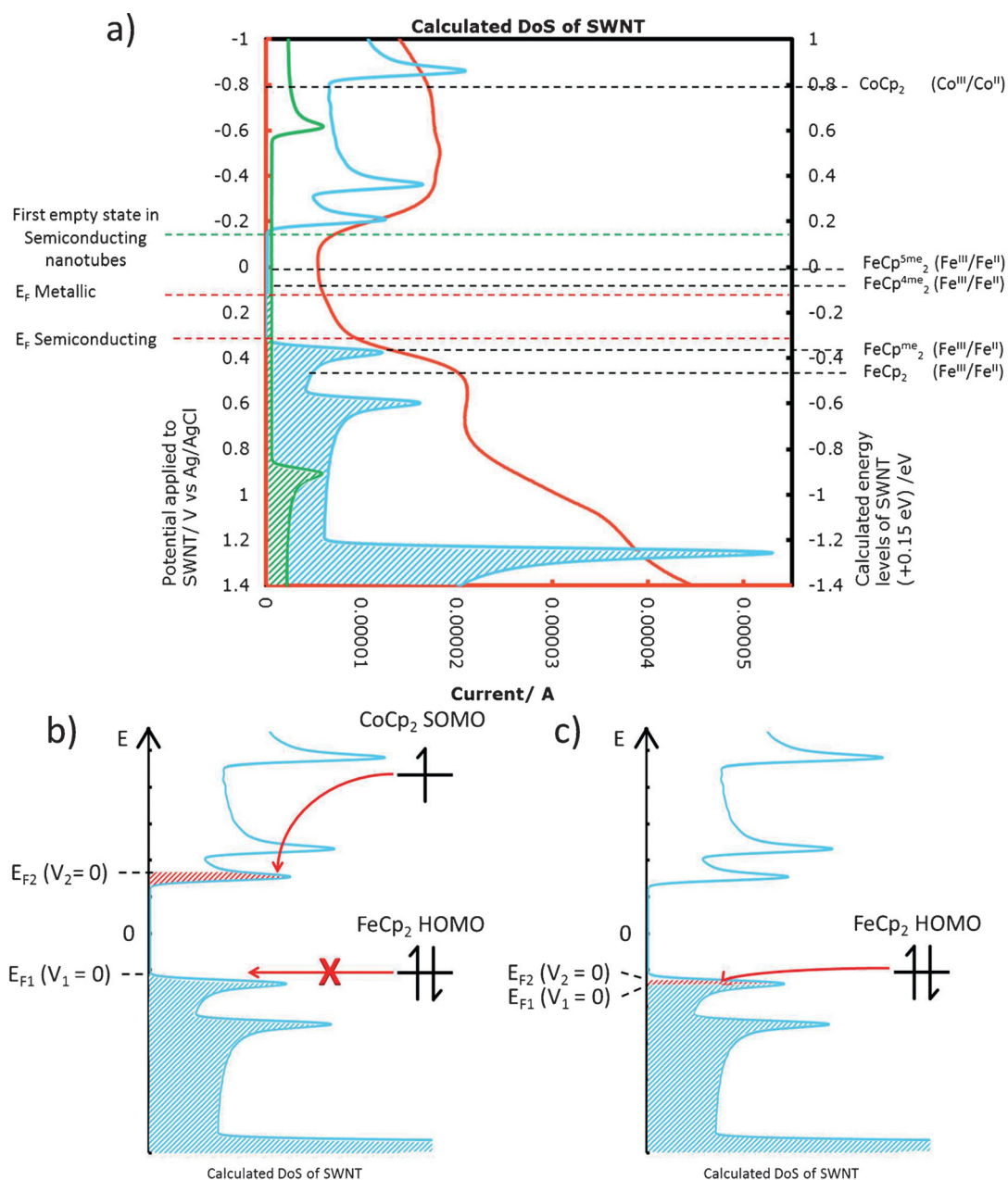


Figure 1. a) Linear-sweep voltammogram (LSV) of empty SWNTs attached to a glassy carbon electrode (GCE; red, red axis) in MeCN containing [NⁿBu₄][BF₄] (0.1 M) as the supporting electrolyte at 293 K and at a scan rate of 100 mV s⁻¹ and DoS of semiconducting (17,0) SWNTs (blue, black axis) and metallic (10,10) SWNTs (green, black axis), representative of the sample calculated by ab initio DFT. The DoS has been shifted by +0.15 eV, as the energy of the DoS is arbitrary with respect to the electrochemical measurement, which is referenced to AgCl/Ag, not absolute potentials. The intensity of the DoS is corrected to represent the ratio of metallic to semiconducting nanotubes in the sample (31:69, metallic/semiconducting)^[33] and the higher number of atoms in the calculation of the wider (17,0) semiconducting SWNTs (204:240 atoms). The Fermi levels (E_F) are marked by a red dashed line and the lowest energy empty state of the (17,0) SWNTs is marked by a green dashed line. The HOMO/SOMO, obtained from the solution CV experiment of selected guest molecules are labelled by black dashed lines. Between -0.10 V and 0.28 V a region of low current is observed at the same position as the band gap shown in the DoS of the (17,0) SWNTs. Increased current is observed at -0.30, 0.50, and 1.10 V, correlating to an increased DoS. b) This shows that electron transfer is possible from the guest molecule to the pristine nanotube in [Co(Cp)₂]@SWNTs but not in [Fe(Cp)₂]@SWNTs due to the position of the energy level of the HOMO/SOMO of the metallocene with respect to the Fermi level and empty nanotube states. As a result of electron transfer from [Co(Cp)₂], the Fermi level of SWNTs (and therefore the zero potential) changes to the new Fermi level E_{F2}. c) In reality, the majority of SWNTs are slightly p-doped,^[34,35] so a small amount of electron transfer from [Fe(Cp)₂] to the SWNTs may take place.

of the valence band of the SWNTs (Figure 1c). Furthermore, the host nanotube partially screens the guest molecule from the solvent, so that effects of the different solvents on the redox potential of [Fe(Cp)₂] inside the nanotube are dampened

(see the Supporting Information). Although confinement in nanotubes has a definite and measurable impact on ferrocene, the fundamental redox properties of [Fe(Cp)₂] inside the nanotube largely remain similar to the properties of the free mole-

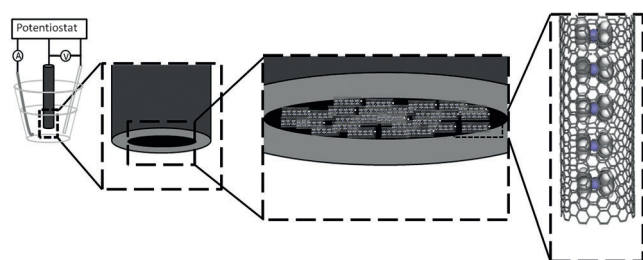


Figure 2. Schematic representation of the experimental setup. A three-electrode cell is used with a Ag/AgCl reference electrode, a platinum counter electrode and SWNTs deposited on a glassy carbon working electrode, in which the investigated guest-species (e.g., metallocene molecules) are encapsulated. Only solvent and electrolyte are in solution, and all redox-active guest molecules are confined within the nanotubes.

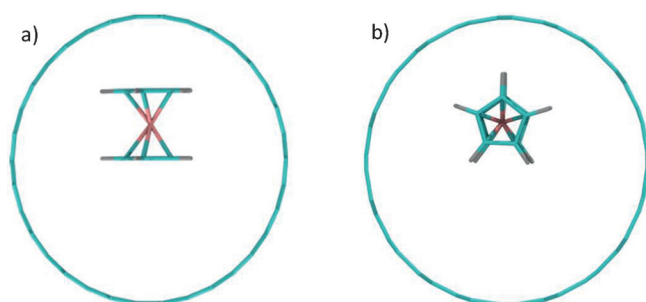


Figure 3. Ab initio geometry-optimised model of $[\text{Fe}(\text{Cp})_2]@(10,10)$ SWNTs in both the perpendicular (a) and parallel (b) orientations.

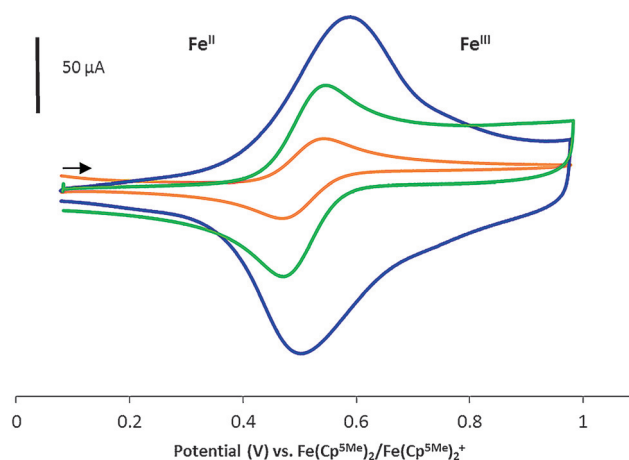


Figure 4. Cyclic voltammograms of $[\text{Fe}(\text{Cp})_2]$ in solution using a GCE ($[\text{Fe}(\text{Cp})_2]/\text{GCE}$; orange), $[\text{Fe}(\text{Cp})_2]$ in solution using a GCE with SWNTs attached ($[\text{Fe}(\text{Cp})_2]/\text{SWNTs}/\text{GCE}$; green) and $[\text{Fe}(\text{Cp})_2]$ encapsulated in SWNTs attached to a GCE ($[\text{Fe}(\text{Cp})_2]@\text{SWNTs}/\text{GCE}$; blue). Arrow denotes sweep direction. All CV experiments were performed in MeCN containing $[\text{N}^i\text{Bu}_4][\text{BF}_4]$ (0.1 M) as the supporting electrolyte at 293 K and a scan rate of 100 mV s^{-1} .

cule in solution, thus indicating that electron transfer plays only a minor role in host–guest interactions in this system.

The magnitude of host–guest electron transfer can change drastically, as demonstrated when cobaltocene $[\text{Co}(\text{Cp})_2]$, with a SOMO much higher than the Fermi level of the SWNTs, is selected as the guest molecule. $[\text{Co}(\text{Cp})_2]$ was successfully insert-

ed into carbon nanotubes by an adaptation of a previously reported method.^[5] Upon encapsulation in SWNTs, the two $[\text{Co}(\text{Cp})_2]$ redox couples, $\text{Co}^{\text{II}}/\text{Co}^{\text{I}}$ and $\text{Co}^{\text{III}}/\text{Co}^{\text{II}}$, are observed. However, both couples occur at significantly shifted potentials when compared to the values obtained for free $[\text{Co}(\text{Cp})_2]$ in solution (Figure 5). It should be noted that the relative currents

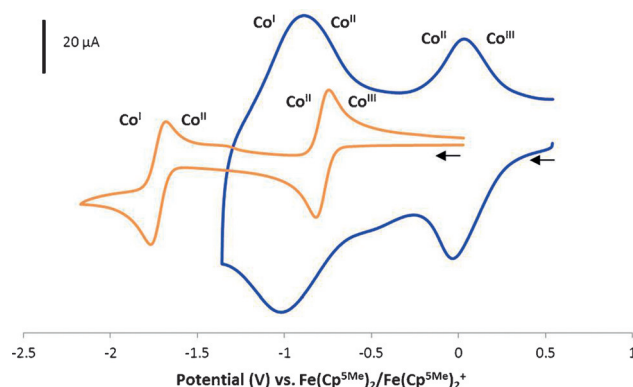


Figure 5. Cyclic voltammograms of $[\text{Co}(\text{Cp})_2]/\text{GCE}$ (orange) and $[\text{Co}(\text{Cp})_2]@\text{SWNTs}/\text{GCE}$ (blue). Arrow denotes sweep direction. All CV experiments were performed in MeCN containing $[\text{N}^i\text{Bu}_4][\text{BF}_4]$ (0.1 M) as the supporting electrolyte at 293 K and a scan rate of 100 mV s^{-1} .

are not equal, as one would expect for two one-electron reductions, due to underlying contributions from the SWNTs energy levels (van Hove singularities) as described in the LSV measurements, which manifest as an uneven non-faradic background in CV measurements.

The observed redox potentials of $[\text{Co}(\text{Cp})_2]@\text{SWNTs}$ of -0.96 V ($\text{Co}^{\text{II}}/\text{Co}^{\text{I}}$) and 0.00 V ($\text{Co}^{\text{III}}/\text{Co}^{\text{II}}$; vs. $[\text{Fe}(\text{Cp}^{5\text{Me}})_2]/[\text{Fe}(\text{Cp}^{5\text{Me}})_2]^+$) are significantly less negative than those observed for $[\text{Co}(\text{Cp})_2]$ in solution, being shifted by $+0.77 \text{ V}$ and $+0.78 \text{ V}$, respectively, and can partly be explained by significant electron transfer from the high-lying $[\text{Co}(\text{Cp})_2]$ SOMO to the nanotube conduction band (Figure 6) so that complete oxidation of cobaltocene to cobaltocenium occurs upon encapsulation. This results in positively charged $[\text{Co}(\text{Cp})_2]$ molecules and negatively charged nanotubes.^[43] A complete electron transfer is not possible with $[\text{Fe}(\text{Cp})_2]$, as the energy of the $[\text{Fe}(\text{Cp})_2]$ HOMO is lower than any empty nanotube states (Figure 1). These CV measurements are in agreement with previously reported spectroscopic measurements for $[\text{Co}(\text{Cp})_2]@\text{SWNTs}$.^[5] Our theoretical calculations also predict the effective injection of an electron from $[\text{Co}(\text{Cp})_2]$ into the nanotube conduction band that results in a shift in energy of the $[\text{Co}(\text{Cp})_2]$ SOMO to a more negative energy by -1.02 eV (more positive potential), which corroborates the shift observed in the CV (Figure 5), in agreement with the calculations reported previously by Sceats and Green.^[10,44]

All cobaltocene molecules inside the SWNTs are positively charged as a result of the electron transfer from cobaltocene to the nanotube. The electron transferred from $[\text{Co}(\text{Cp})_2]$ is delocalised around the extended π system of the nanotube and so dispersed. However, the positive charge of the $[\text{Co}(\text{Cp})_2]^+$

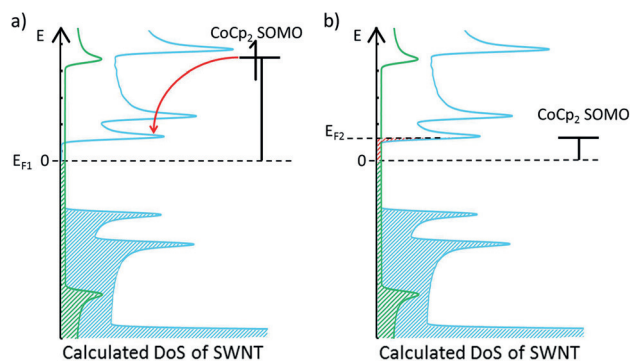


Figure 6. Encapsulation of cobaltocene in SWNTs leads to a shift in the energy of the $[\text{Co}(\text{Cp})_2]$ SOMO^[43] and an effective injection of electrons into the nanotube DoS, increasing the energy of the Fermi level from E_{F1} to E_{F2} . As a result of the electron transfer, the potential required to perform a redox reaction of $[\text{Co}(\text{Cp})_2]$ inside the nanotube is decreased by 0.77 V. This is due to the localised charges on adjacent $[\text{Co}(\text{Cp})_2]$.

molecule is localised on the encapsulated molecule, which is adjacent to other positively charged $[\text{Co}(\text{Cp})_2]^+$ molecules. The overriding force that influences an encapsulated $[\text{Co}(\text{Cp})_2]$ molecule is the concentrated positive charges of adjacent $[\text{Co}(\text{Cp})_2]^+$ rather than the dispersed negative charge on the nanotube (Figure 7). The consequence of these positive charg-

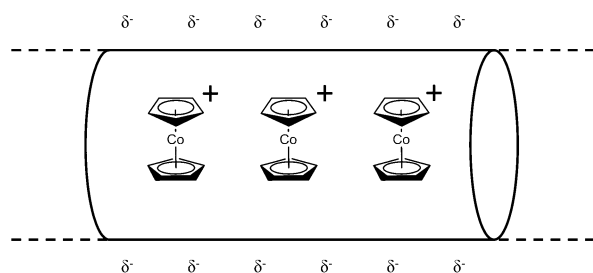


Figure 7. Schematic representation of $[\text{Co}(\text{Cp})_2]$ @SWNTs, demonstrating the location of charges. The charge transfer from $[\text{Co}(\text{Cp})_2]$ to the SWNT results in a dispersed negative charge on the nanotube and a concentrated positive charge on $[\text{Co}(\text{Cp})_2]$.

es is to stabilise the molecular orbitals of $[\text{Co}(\text{Cp})_2]$, hence, the observed shift in potential of the redox processes $\text{Co}^{\text{II}}/\text{Co}^{\text{I}}$ and $\text{Co}^{\text{III}}/\text{Co}^{\text{II}}$ of $[\text{Co}(\text{Cp})_2]$ is in the positive direction. A shift is not observed with $[\text{Fe}(\text{Cp})_2]$, as there is only a minor electron transfer to the nanotube and so $[\text{Fe}(\text{Cp})_2]$ is not positively charged inside the nanotube. Therefore, although the interaction of the nanotube with $[\text{Co}(\text{Cp})_2]$ is initiated by the charge transfer of an electron from $[\text{Co}(\text{Cp})_2]$ to the nanotube, the shift in redox potential of the $[\text{Co}(\text{Cp})_2]$ reductions is attributed to the positive charges on adjacent $[\text{Co}(\text{Cp})_2]^+$.

Ferrocene and cobaltocene represent two extreme cases for which the magnitudes of electron transfer to the nanotube are very low and very high, respectively. To explore whether electron transfer between the host and the guest can be finely tuned through size, shape, functionality, and electronic structure of the guest molecule, a series of methylated $[\text{Fe}(\text{Cp})_2]$ de-

rivatives with a varying number of methyl groups on the cyclopentadienyl (Cp) ring, were encapsulated in SWNTs.

The introduction of an increasing number of methyl groups into $[\text{Fe}(\text{Cp})_2]$ (zero to ten) increases the energy of the HOMO ($E_{1/2}$ occurs at a less positive potential) and therefore increases the observed shift in the redox process (from 0.04 V for $[\text{Fe}(\text{Cp})_2]$ to 0.20 V for $[\text{Fe}(\text{Cp}^{5\text{Me}})_2]$) for the guest molecule inside the nanotube of each $[\text{Fe}(\text{Cp}^X)_2]$ @SWNT ($X = \text{Me}, 4\text{Me}, 5\text{Me}$) system (see the Supporting Information). The energy of the ferrocene HOMO increases with the number of methyl groups, owing to a well-known inductive effect, so a greater number of methyl groups on the molecule lead to more electron density transferred to the host nanotube. Whereas the HOMOs for $[\text{Fe}(\text{Cp})_2]$ and $[\text{Fe}(\text{Cp}^{\text{Me}})_2]$ are high enough in energy to enable a small amount of electron transfer to p-doped semiconducting nanotubes (Figure 1c), the addition of 8 and 10 methyl groups increases the HOMO energy of $[\text{Fe}(\text{Cp}^{4\text{Me}})_2]$ and $[\text{Fe}(\text{Cp}^{5\text{Me}})_2]$ to above the Fermi level of the metallic (10,10) nanotubes. Therefore, electron transfer no longer relies on the p-doped nanotubes but a transfer to the conduction band of metallic nanotubes, resulting in a sharp increase in electron transfer, measured as a shift in the redox potential of the guest molecule (Figure 1a, Table 1). In general, the shift of

Table 1. Comparison of the calculated ΔE of encapsulation for different ferrocene molecules in a (17,0) SWNT to the shift in redox process of the guest molecules detected by CV experiments.

Guest molecule	ΔE of encapsulation [eV] ^[a]	Shift in redox potential [V] ^[b]
$[\text{Fe}(\text{Cp})_2]$	0.00	0.04
$[\text{Fe}(\text{Cp}^{\text{Me}})_2]$	-0.02	0.05
$[\text{Fe}(\text{Cp}^{4\text{Me}})_2]$	-0.16	0.18
$[\text{Fe}(\text{Cp}^{5\text{Me}})_2]$	-0.26	0.20

[a] Vs. $[\text{Fe}(\text{Cp})_2]$ @(17,0) SWNTs; [b] encapsulated vs. free molecule.

redox potential can be interpreted as a measure of charge transfer from the guest molecule to the host nanotube and an increase in positive charge on the guest molecule, therefore, is related to the strength of host-guest interactions. The clear correlation between redox potential shift and electron-donating ability of the metallocenes further indicates that the nature of the interactions with SWNTs is primarily electrostatic, unlike in the case of fullerene, where van der Waals interactions dominate.

Ab initio DFT calculations were carried out to corroborate the link between the strength of host-guest interactions and electron transfer (see the Supporting Information). The calculated energies of encapsulation ΔE [defined as $\Delta E = E(\text{metallocene@SWNT}) - E(\text{metallocene}) - E(\text{SWNT})$] for different ferrocene molecules in SWNTs correlate well with the experimentally measured shifts in redox potential for the different metallocenes upon nanotube confinement (Table 1). This is a strong indication that the electron transfer from metallocenes to the nanotube results in a stronger interaction with the internal cavity of the SWNTs, which gives us a mechanism to gauge not only the nature of the interaction between the nanotube

and the guest molecule but also the strength of the interaction using electrochemical methods.

Our CV measurements revealed that the internal diameter of the host nanotube also has an effect on the magnitude of the shift of the $E_{1/2}$ of $[\text{Fe}(\text{Cp})_2]$, with the observed shift ranging from 0.05 V for the narrowest nanotubes ($d_{\text{NT}}=1.0$ nm) to 0.01 V for the widest nanotubes studied ($d_{\text{NT}}=2.5$ nm) and appears to be inversely proportional to the nanotube diameter (see the Supporting Information). Nanotubes with a narrow diameter have a wider band gap resulting in the top of the valence band residing at a lower energy. Assuming that as-received SWNTs are slightly p-doped, the Fermi level of a narrower nanotube will be at a lower energy, facilitating electron transfer from $[\text{Fe}(\text{Cp})_2]$ to the nanotube, which further proves that the electrostatic forces, which determine the effectiveness of host–guest interactions, rely on electron transfer from the guest molecule to the host nanotube.

Although the use of CV experiments to detect precise changes in redox processes can be a useful measure of the redox state of guest molecules within nanotubes, these experiments provide very limited information about the electronic state of the host nanotube in terms of the amount of electron density injected into the SWNTs from guest molecules or the actual position of the Fermi level in the metallocene@nanotube system. To answer these fundamentally important questions, a new type of experimental procedure has been developed and applied to the metallocene-filled carbon nanotubes.

A series of different potentials were applied to empty SWNTs attached to a glassy carbon electrode in an electrochemical cell (Figure 2) and the resultant charge was measured across a potential range that encompasses the nanotube Fermi level. Consequently, the current generated at a given potential applied to the nanotubes is proportional to the density of SWNT electronic states at that particular energy, allowing accurate mapping of the states that are filled or emptied upon application of a specific potential. Negative or positive charge registered by the potentiostat corresponds to electrons moving to or from the nanotubes, respectively (Figure 8). Importantly, zero charge signifies the absence of any electronic states in the SWNTs at that particular applied potential (resulting in a so-called resting potential window). Therefore, although the coulometry relates well to the LSV measurements (Figure 1a), this method also reveals important information about the electronic state of the host nanotube, particularly around the Fermi energy, and measures the states without prior perturbation of the guest@SWNTs ground state, unlike in CV. Thus, if the range of applied potentials falls within the bandgap of the SWNTs, little or no charge will be registered, which enables quantification of the size of the nanotube bandgap with the accuracy limited solely by the size of the steps in applied potential. The potential at which the first positive charge is observed indicates the position of the top of the valence band and can therefore be correlated with the Fermi level of the SWNTs, whereas the potential at which the first negative charge is observed corresponds to the first empty state of the SWNTs (i.e., the bottom of the conduction band). In our experiments, empty SWNTs exhibit a low-charge region between

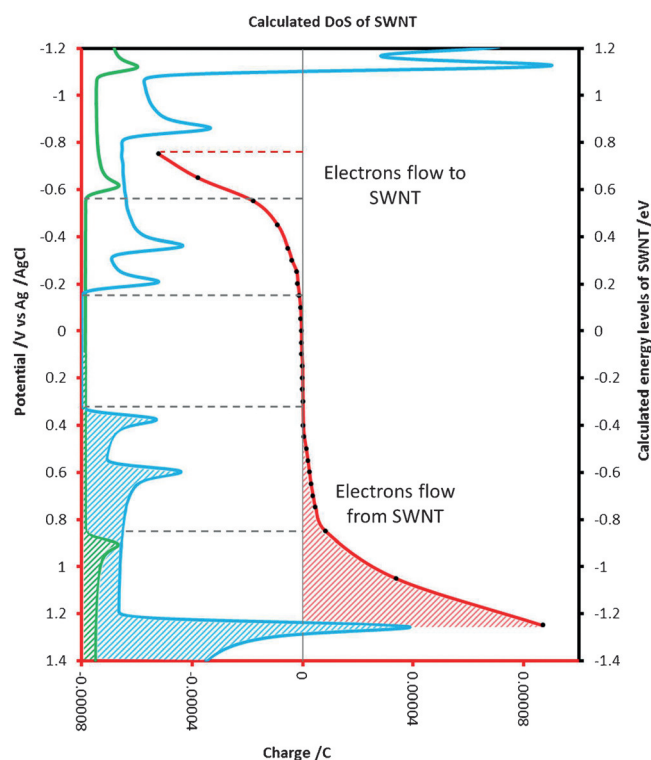


Figure 8. Coulometry measurements at a series of potentials around the Fermi level of empty SWNTs (red curve, red axes) and DoS of semiconducting (17,0) SWNTs (blue curve, black axes) and metallic (10,10) SWNTs (green curve, black axes) calculated by ab initio DFT. The shaded area under the coulometry curve represents charge generated due to electrons being removed from the SWNTs (positive charge), the unshaded area represents electrons flowing into the SWNTs from the electrode (negative charge) and the grey dashed lines indicate significant features in the calculated DoS. The experiment was performed in MeCN containing $[\text{N}^{\text{t}}\text{Bu}_4][\text{BF}_4]$ (0.1 M) as the supporting electrolyte at 293 K and the amount of transferred charge was measured for 40 s at each applied potential. The DoS of the nanotubes is corrected to match the typical ratio of metallic to semiconducting nanotubes in the sample (31:69, metallic/semiconducting)^[33] and the higher number of atoms in the calculation of the wider (17,0) SWNTs (204:240 atoms). A resting potential window (zero or low charge) observed in the coulometry curve matches the bandgap of semiconducting nanotubes and a sharp increase in current is observed when the applied potential is set in the region of high nanotube DoS (e.g., the van Hove singularities).

–0.11 V and 0.40 V in the coulometry experiment, which is characteristic of the bandgap of semiconducting nanotubes predominant in this sample^[38] and corresponds well to calculations (Figure 8). The same methodology was then utilised to explore the electronic band structure of the nanotubes filled with molecules, $[\text{Fe}(\text{Cp})_2]$ @SWNTs (Figure 9) and $[\text{Co}(\text{Cp})_2]$ @SWNTs (Figure 10). The coulometric $[\text{Fe}(\text{Cp})_2]$ @SWNTs curve is similar to that for SWNTs but with a resting potential window that is 0.23 V narrower than that for the empty nanotubes (Figure 9), whereas $[\text{Co}(\text{Cp})_2]$ @SWNTs shows no resting potential window with the charge only reaching zero at a potential of 0 V, which is the position of the Fermi level, implying that the nanotubes in $[\text{Co}(\text{Cp})_2]$ @SWNTs effectively do not possess a bandgap. Furthermore, the coulometric behaviour of nanotubes filled with methylated ferrocenes, $[\text{Fe}(\text{Cp}^{\text{Me}})_2]$ @SWNTs and $[\text{Fe}(\text{Cp}^{\text{Me}_2})_2]$ @SWNTs, appear to be inter-

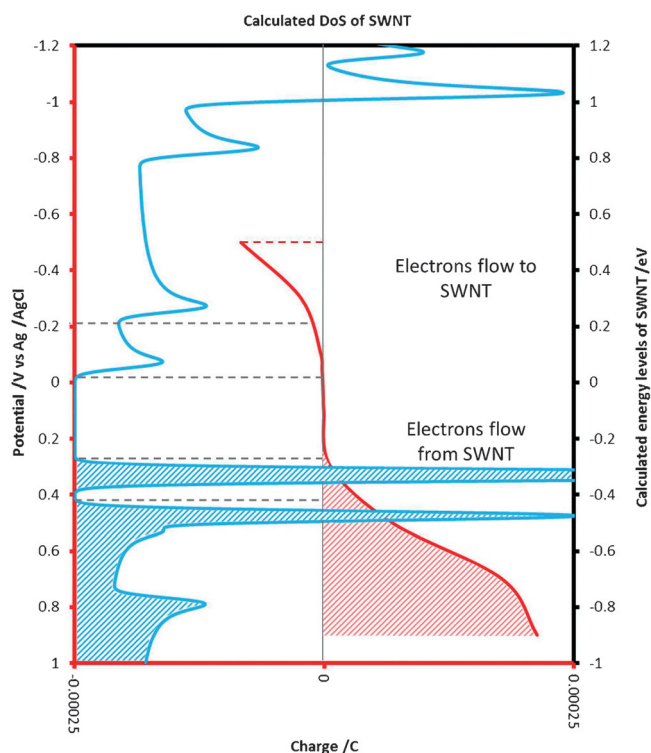


Figure 9. Coulometry measurements at a series of potentials for $[\text{Fe}(\text{Cp})_2]@\text{SWNTs}$ (red curve, red axis) and DoS of $[\text{Fe}(\text{Cp})_2]@(17,0)$ SWNTs where $[\text{Fe}(\text{Cp})_2]$ is in a perpendicular orientation to the nanotube (blue curve, black axis) calculated by ab initio DFT. The shaded area under the coulometry curve represents charge generated due to electrons being removed from the SWNTs (positive charge), the unshaded area represents electrons flowing into the SWNTs from the electrode (negative charge) and the grey dashed lines indicate significant features in the calculated DoS. The experiment was performed in MeCN containing $[\text{N}^{\text{t}}\text{Bu}_4][\text{BF}_4]$ (0.1 M) as the supporting electrolyte at 293 K and the amount of transferred charge was measured for 40 sec at each applied potential. The sharp increases in DoS at 0.35 V and 0.50 V originate from $[\text{Fe}(\text{Cp})_2]$ orbitals just below the Fermi level, which, along with partial electron transfer from the guest molecule, leads to the observed narrowing of the resting potential window.

mediate between $[\text{Fe}(\text{Cp})_2]@\text{SWNTs}$ and $[\text{Co}(\text{Cp})_2]@\text{SWNTs}$, with the resting potential window becoming narrower as the number of methyl groups increases (see the Supporting Information).

These observations can be rationalised by considering the nature and electronic configuration of the guest species within the nanotubes. For example the energy of the $[\text{Fe}(\text{Cp})_2]$ HOMO is lower than the Fermi level of the host nanotube so electrons can only be transferred into the holes in the valence band created by p-doping as described earlier (Figure 1 b,c). Therefore, even though the encapsulation of $[\text{Fe}(\text{Cp})_2]$ does not significantly change the density of electrons on the nanotube, the apparent bandgap of $[\text{Fe}(\text{Cp})_2]@\text{SWNTs}$ (measured as the resting potential window) becomes smaller due to $[\text{Fe}(\text{Cp})_2]$ molecular orbital states (HOMO) at about 0.3 V (Figure 9). In contrast, $[\text{Co}(\text{Cp})_2]$ is a strong electron donor with a high energy SOMO. Upon encapsulation a significant amount of electron density is transferred from $[\text{Co}(\text{Cp})_2]$ to the SWNTs, as demonstrated in our CV measurements, leading to an increase in the energy of the Fermi level into the conduction band of the nanotube (i.e.,

above the intrinsic bandgap of SWNTs (Figure 10). This results in the electronic structure of $[\text{Co}(\text{Cp})_2]@\text{SWNTs}$ containing high density of states either side of the Fermi level which explains the absence of resting potential window in the coulometry of this material. Interestingly a lower rate of electron transfer from $[\text{Co}(\text{Cp})_2]@\text{SWNTs}$ to the electrode in the potential range -0.5 to 0 V is observed due to the relatively low DoS of electron-doped metallic nanotubes in this range, as compared to a higher rate of electron transfer from the electrode to $[\text{Co}(\text{Cp})_2]@\text{SWNTs}$ between 0.5 V and 0.9 V, due to a much higher density of empty states just above the Fermi level in this material (Figure 10).

Nanotubes filled with methylated ferrocenes which have a HOMO of increasing energy as the number of methyl groups increases (Figure 1) follow the trend of a narrowing band gap (e.g., decreasing the resting potential window in coulometry). The impact of the guest molecule on the host nanotube is more pronounced for $[\text{Fe}(\text{Cp}^{4\text{Me}})_2]$ and $[\text{Fe}(\text{Cp}^{5\text{Me}})_2]$ because their HOMO energy is sufficiently high for their valence electrons to be transferred to the empty states of the metallic nanotubes as well as the p-doped semiconducting nanotubes in the sample (see the Supporting Information), however, the HOMO of $[\text{Fe}(\text{Cp}^{4\text{Me}})_2]$ and $[\text{Fe}(\text{Cp}^{5\text{Me}})_2]$ are not high enough to n-dope the semiconducting nanotubes as in the case of $[\text{Co}(\text{Cp})_2]$.

Coulometry allows accurate determination of the electronic band structure of the SWNTs around the Fermi level of nanotubes filled with guest molecules, providing important information about the nature of electron transfer between the molecule and nanotube. However, coulometry on its own does not provide quantitative information about the extent of any electron transfer processes. This can only be achieved by considering the exact value of the redox potential (HOMO/SOMO energy) of the specific guest molecules in nanotubes measured by CV experiments of the specific guest in solution. Our coulometry measurements quantitatively establish the Fermi levels of empty metallic and semiconducting nanotubes (Figure 8), and therefore the potential experienced by any guest molecule encapsulated in a host nanotube, as 0.13 V and -0.11 V (vs. Ag/AgCl) respectively. The Fermi level of the metallic nanotubes is determined to be the potential at which the charge is zero. The first empty state of semiconducting nanotubes is the first measured negative charge, which is the bottom of the conduction band. These potentials (0.13 V and -0.11 V) are the oxidising potentials applied by the SWNTs on encapsulated molecules in the absence of any external potential (Figure 8). Correlation of the guest molecule HOMO/SOMO energy with the Fermi level of the host nanotube by using the Nernst equation provides an estimate of the percentage of molecules that transfer their valence electrons to the nanotube (Table 2). A similar method was applied previously for a series of salts on a graphene crystal.^[45] For example, the Nernst equation applied to $[\text{Fe}(\text{Cp})_2]@\text{SWNTs}$ and $[\text{Fe}(\text{Cp}^{\text{Me}})_2]@\text{SWNTs}$ predicts no measurable electron transfer to the nanotube, so the majority of these guest molecules remain unchanged upon encapsulation, which is consistent with the CV measurements for these materials. The same calculation for $[\text{Co}(\text{Cp})_2]@\text{SWNTs}$ results in

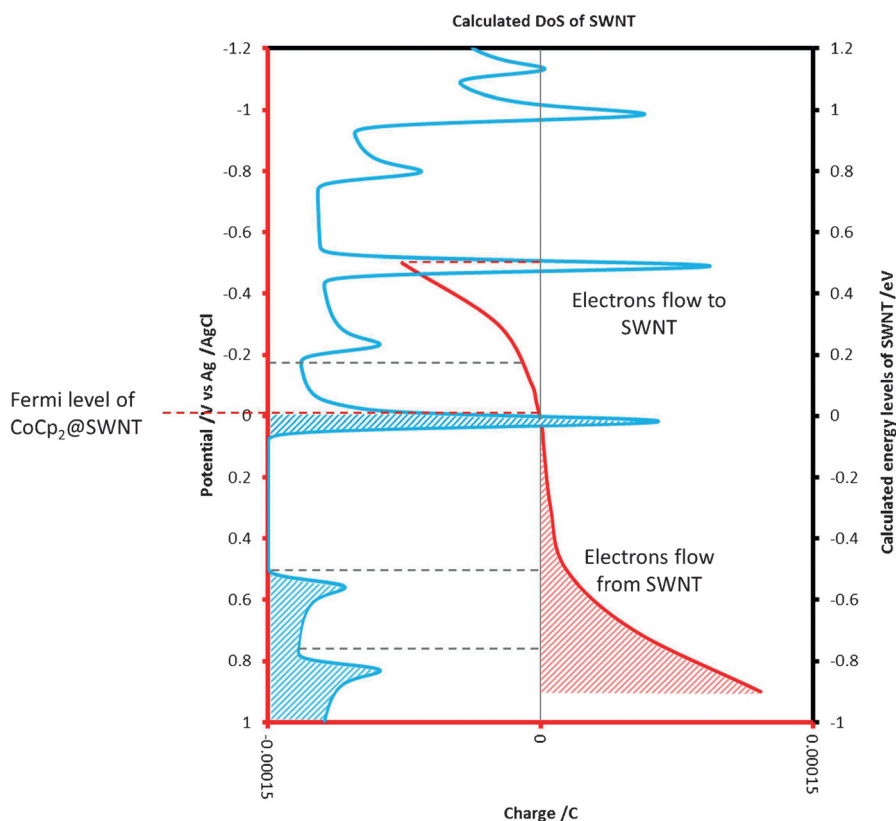


Figure 10. Coulometry measurements at a series of potentials for $[\text{Co}(\text{Cp})_2]@\text{SWNTs}$ (red curve, red axis) and DoS of $[\text{Co}(\text{Cp})_2]@(17,0)$ SWNTs where $[\text{Co}(\text{Cp})_2]$ is in a perpendicular orientation to the nanotube (blue curve, black axis) calculated by ab initio DFT. The shaded area under the coulometry curve represents charge generated due to electrons being removed from the SWNTs (positive charge), the unshaded area represents electrons flowing into the SWNTs from the electrode (negative charge) and the grey dashed lines indicate significant features in the calculated DoS. The experiment was performed in MeCN containing $[\text{N}^n\text{Bu}_4][\text{BF}_4]$ (0.1 M) as the supporting electrolyte at 293 K and the amount of transferred charge was measured for 40 s at each applied potential. The sharp increases in DoS at 0.00 V and -0.50 V originate from the $[\text{Co}(\text{Cp})_2]$ orbitals. The significant electron transfer from $[\text{Co}(\text{Cp})_2]$ to the SWNTs results in mixing of the host and guest orbitals, thus raising the Fermi level above the intrinsic nanotube bandgap.

a complete electron transfer from the guest $[\text{Co}(\text{Cp})_2]$ to the nanotube, which is again consistent with the CV for this structure. Interestingly, the predicted behaviours of $[\text{Fe}(\text{Cp}^{4\text{Me}})_2]$ and $[\text{Fe}(\text{Cp}^{5\text{Me}})_2]$ guest molecules fall between those of ferrocene and cobaltocene, as, according to the Nernst equation, the methylated ferrocene molecules are able to transfer a valence electron to metallic SWNTs but not to semiconducting SWNTs (Table 2).

These values correlate well with our CV measurements for guest@SWNT systems to probe the oxidation state of the guest

molecules: the small percentage of electron transfer from $[\text{Fe}(\text{Cp})_2]$ and $[\text{Fe}(\text{Cp}^{\text{Me}})_2]$ to the nanotube predicted by the Nernst equation is matched by the small shift observed in the redox potential of $[\text{Fe}(\text{Cp})_2]@\text{SWNT}$ and $[\text{Fe}(\text{Cp}^{\text{Me}})_2]@\text{SWNT}$ as compared to the molecule in solution (Table 1). The high percentage of electron transfer from $[\text{Co}(\text{Cp})_2]$ to the nanotube matches a big shift in the redox potential of $[\text{Co}(\text{Cp})_2]@\text{SWNT}$. The guest molecules $[\text{Fe}(\text{Cp}^{5\text{Me}})_2]$ and $[\text{Fe}(\text{Cp}^{4\text{Me}})_2]$ represent a special case, as they are able to transfer electrons to the metallic nanotubes present in the sample, but not to the majority

Table 2. Percentage of guest species that transfer an electron to the nanotube in a bulk sample, as estimated by the Nernst equation.^[a]

Guest molecule ^[b]	Transfer to metallic nanotubes [%]	Transfer to semiconducting nanotubes [%]	Overall electron transfer in sample [%] ^[c,d]	Average oxidation state of metal in sample
$[\text{Fe}(\text{Cp})_2]$ (0.00 V)	2×10^{-4}	0	7×10^{-5}	+2.00
$[\text{Fe}(\text{Cp}^{\text{Me}})_2]$ (-0.10 V)	1×10^{-2}	0	4×10^{-3}	+2.00
$[\text{Fe}(\text{Cp}^{4\text{Me}})_2]$ (-0.41 V)	96.1	0.2	30.0	+2.30
$[\text{Fe}(\text{Cp}^{5\text{Me}})_2]$ (-0.46 V)	99.4	1.1	31.6	+2.32
$[\text{Co}(\text{Cp})_2]$ (-1.27 V)	100.0	100.0	100	+3.00

[a] The Fermi level potentials of metallic and semiconducting nanotubes are 0.13 V and -0.11 V (vs. Ag/AgCl) respectively; [b] the redox potential of the free molecule (i.e., in solution) is listed vs. $[\text{Fe}(\text{Cp})_2]^+ / [\text{Fe}(\text{Cp})_2]$ in parentheses; [c] calculated assuming a ratio of metallic/semiconducting nanotubes of 31:69;^[7] [d] the number of significant figures is beyond the accuracy of the measurement and is given to show that there are very small amounts of electron transfer with some combinations of nanotubes and molecules.

of semiconducting nanotubes (Table 2), which also correlates with the shifts of their redox potential inside the SWNTs, as measured by CV (Table 1). As a result, within the samples of $[\text{Fe}(\text{Cp}^{5\text{Me}})_2]@\text{SWNTs}$ and $[\text{Fe}(\text{Cp}^{4\text{Me}})_2]@\text{SWNTs}$, there will be molecules that have transferred an electron to the host nanotube and those that remained unchanged upon encapsulation, depending on whether the host nanotube is metallic or semiconducting, respectively. Within this framework of considerations, combining cyclic voltammetry and coulometry data according to the Nernst equation enables the determination of the precise oxidation state of guest molecules in carbon nanotubes.

Conclusion

We have developed a powerful methodology based on electrochemical analysis that allows probing of the mechanisms of interactions between redox active guest molecules and carbon nanotubes. Specifically, coulometry was used to reveal the impact of guest molecules on the electronic levels of the host nanotube, and cyclic voltammetry, combined with information about the actual Fermi level in the molecule@SWNTs system obtained from coulometry, was used to determine the real oxidation state of the guest molecule. Although a *priori* prediction and spectroscopic measurements of the oxidation states of guest molecules in carbon nanotubes are difficult, our electrochemical approach determined them with great precision. Our study demonstrates a complex interplay between the molecular orbitals of guest molecules with the electronic bands of host nanotubes. Encapsulation of redox-active guest molecules triggers electron transfer to the nanotube, the extent of which depends on several parameters: the energy of HOMO/SOMO of the guest molecule, the diameter of the nanotube, and whether the nanotube is metallic or semiconducting. This new knowledge significantly improves our understanding of host-guest interactions and opens up new avenues for controlling the oxidation state of guest molecules, as well as for tuning the electronic properties of host nanotubes.

Experimental Section

Reagents and solvents were purchased from Sigma Aldrich, Acros and Alfa Aesar and were used without further purification. Carbon nanotubes were purchased from Carbon Solutions (P2-SWNTs, Carbon Solutions Inc., USA, lot#: 02-A006, carbonaceous purity: >90%), Chengdu Organic Chemicals Co. and NanoIntegris Inc. $[\text{Fe}(\text{Cp}^{5\text{Me}})_2]@\text{SWNTs}$ (1.4 nm diameter) materials were prepared using a previously reported method,^[41] whereas $[\text{Co}(\text{Cp})_2]@\text{SWNTs}$ (1.4 nm diameter) was prepared by an adaptation of a reported procedure.^[5] Further details are given in the Supporting Information.

Electrochemistry

Electrodes were 3 mm diameter glassy carbon disc sheathed in polyether ether ketone (PEEK). A three-electrode setup was used with a Ag/AgCl reference electrode, a platinum counter electrode, and SWNTs deposited on a glassy carbon working electrode (GCE), in which the investigated species was encapsulated. Electrochemistry experiments were performed using an Autolab PGSTAT302N po-

tentiostat. For CV the potential was held at the starting potential for 5 seconds prior to experiment.

Electrode fabrication

Guest@nanotubes (0.5 mg) was sonicated (15 min) in dry DMF (0.5 mL) to form an ink. 10 μL of the ink was cast onto the GCE using a micropipette and allowed to dry in air for 1 h. The electrode was then rinsed in dry MeCN and allowed to dry in air.

Coulometry experiments

A series of potentials ($-0.75\text{ V} \rightarrow 1.25\text{ V}$, with steps of 0.05 V close to the Fermi level and steps of 0.10 V for empty SWNTs or 0.20 V for guest@SWNTs for potentials associated with the valence and conduction bands) that encompass the Fermi level were applied to $[\text{Fe}(\text{Cp}^{x\text{Me}})_2]@\text{SWNTs}/\text{GCE}$ for 40 s and the charge measured. A period of 2 h was left between the application of each potential to allow the nanotube sample to return to its ground state (see the Supporting Information). Experiments were performed in MeCN at 293 K containing $[\text{N}^i\text{Bu}_4][\text{BF}_4]$ (0.1 M) as the supporting electrolyte at a scan rate of 100 mVs^{-1} .

Electron microscopy

HRTEM analysis was performed on a JEOL JEM-2100F FEG electron microscope with an information limit of 0.12 nm at 100 kV. The imaging conditions were carefully tuned by lowering the accelerating voltage of the microscope to 100 kV and lowering the beam current density to a minimum to avoid electron beam damage on the specimen. Suspensions of guest@nanotube in HPLC-grade isopropanol were drop cast onto lacey carbon grids for TEM analysis.

Acknowledgements

This work was supported by the European Research Council (ERC), the Engineering, Physical Sciences Research Council (EPSRC), the University of Nottingham, and Russian Federation Ministry of Science and Education Grant Nr. K3-2015-030 (MISIS). We thank the Nanoscale & Microscale Research Centre (NMRC) for access to electron microscopy facilities and the High-Performance Computing Facility (HPC) at the University of Nottingham for access to computing resources.

Keywords: carbon nanotubes • charge transfer • electrochemistry • host-guest systems • metallocenes

- [1] T. W. Chamberlain, T. Zoberbier, J. Biskupek, A. Botos, U. Kaiser, A. N. Khlobystov, *Chem. Sci.* **2012**, *3*, 1919–1924.
- [2] W. A. Solomonsz, G. A. Rance, B. J. Harris, A. N. Khlobystov, *Nanoscale* **2013**, *5*, 12200–12205.
- [3] D. A. Britz, A. N. Khlobystov, *Chem. Soc. Rev.* **2006**, *35*, 637–659.
- [4] X. Pan, X. Bao, *Acc. Chem. Res.* **2011**, *44*, 553–562.
- [5] L. J. Li, A. N. Khlobystov, J. G. Wiltshire, G. A. Briggs, R. J. Nicholas, *Nat. Mater.* **2005**, *4*, 481–485.
- [6] S. A. Miners, G. A. Rance, A. N. Khlobystov, *Chem. Commun.* **2013**, *49*, 5586–5588.
- [7] P. Kim, T. W. Odom, J. L. Huang, C. M. Lieber, *Phys. Rev. Lett.* **1999**, *82*, 1225–1228.
- [8] T. W. Odom, J. L. Huang, P. Kim, C. M. Lieber, *J. Phys. Chem. B* **2000**, *104*, 2794–2809.
- [9] T. Fukumaru, T. Fujigaya, N. Nakashima, *Sci. Rep.* **2015**, *5*, 7951.
- [10] E. L. Scaets, J. C. Green, *J. Chem. Phys.* **2006**, *125*, 154704.

- [11] D. M. Guldi, G. M. A. Rahman, F. Zerbetto, M. Prato, *Acc. Chem. Res.* **2005**, *38*, 871–878.
- [12] M. Sauer, H. Shiozawa, P. Ayala, G. Ruiz-Soria, X. J. Liu, A. Chernov, S. Krause, K. Yanagi, H. Kataura, T. Pichler, *Carbon* **2013**, *59*, 237–245.
- [13] K. Yanagi, R. Moriya, N. T. Cuong, M. Otani, S. Okada, *Phys. Rev. Lett.* **2013**, *110*, 086801.
- [14] T. S. Miller, N. Ebejer, A. G. Guell, J. V. Macpherson, P. R. Unwin, *Chem. Commun.* **2012**, *48*, 7435–7437.
- [15] A. G. Güell, K. E. Meadows, P. V. Dudin, N. Ebejer, J. V. Macpherson, P. R. Unwin, *Nano Lett.* **2014**, *14*, 220–224.
- [16] R. L. McSweeney, T. W. Chamberlain, E. S. Davies, A. N. Khlobystov, *Chem. Commun.* **2014**, *50*, 14338–14340.
- [17] Z. D. Chang, N. S. Gao, Y. J. Li, X. W. He, *Anal. Methods* **2012**, *4*, 4037–4041.
- [18] J. E. Halls, A. Hernan-Gomez, A. D. Burrows, F. Marken, *Dalton Trans.* **2012**, *41*, 1475–1480.
- [19] C. A. Bessel, D. R. Rolison, *J. Am. Chem. Soc.* **1997**, *119*, 12673–12674.
- [20] G. H. Clever, S. Tashiro, M. Shionoya, *Angew. Chem. Int. Ed.* **2009**, *48*, 7010–7012; *Angew. Chem.* **2009**, *121*, 7144–7146.
- [21] W. Y. Sun, T. Kusukawa, M. Fujita, *J. Am. Chem. Soc.* **2002**, *124*, 11570–11571.
- [22] C. M. Cardona, S. Mendoza, A. E. Kaifer, *Chem. Soc. Rev.* **2000**, *29*, 37–42.
- [23] M. V. Kharlamova, M. Sauer, T. Saito, Y. Sato, K. Suenaga, T. Pichler, H. Shiozawa, *Nanoscale* **2015**, *7*, 1383–1391.
- [24] A. J. Bard, L. R. Faulkner, *Electrochemical Methods: Fundamentals and Applications*, John Wiley and Sons, Inc., Hoboken, NJ, **2001**.
- [25] H. Ulbricht, G. Moos, T. Hertel, *Phys. Rev. Lett.* **2003**, *90*, 095501.
- [26] A. N. Khlobystov, D. A. Britz, J. W. Wang, S. A. O’Neil, M. Poliakoff, G. A. D. Briggs, *J. Mater. Chem.* **2004**, *14*, 2852–2857.
- [27] L. A. Girifalco, M. Hodak, R. S. Lee, *Phys. Rev. B* **2000**, *62*, 13104–13110.
- [28] M. A. Lebedeva, T. W. Chamberlain, M. Schröder, A. N. Khlobystov, *Chem. Mater.* **2014**, *26*, 6461–6466.
- [29] W. A. Solomonsz, G. A. Rance, A. N. Khlobystov, *Small* **2014**, *10*, 1866–1872.
- [30] X. Pan, X. Bao, *Chem. Commun.* **2008**, 6271–6281.
- [31] C. del Carmen Giménez-López, F. Moro, A. La Torre, C. J. Gomez-Garcia, P. D. Brown, J. van Slageren, A. N. Khlobystov, *Nat. Commun.* **2011**, *2*, 407.
- [32] H. M. Cheng, H. X. Qiu, Z. W. Zhu, M. X. Li, Z. J. Shi, *Electrochim. Acta* **2012**, *63*, 83–88.
- [33] S. Cambré, W. Wenseleers, E. Goovaerts, D. E. Resasco, *ACS Nano* **2010**, *4*, 6717–6724.
- [34] J. Vavro, M. C. Llaguno, J. E. Fischer, S. Ramesh, R. K. Saini, L. M. Ericson, V. A. Davis, R. H. Hauge, M. Pasquali, R. E. Smalley, *Phys. Rev. Lett.* **2003**, *90*, 065503.
- [35] Y. Iizumi, H. Suzuki, M. Tange, T. Okazaki, *Nanoscale* **2014**, *6*, 13910–13914.
- [36] I. Heller, J. Kong, H. A. Heering, K. A. Williams, S. G. Lemay, C. Dekker, *Nano Lett.* **2005**, *5*, 137–142.
- [37] I. Heller, J. Kong, K. A. Williams, C. Dekker, S. G. Lemay, *J. Am. Chem. Soc.* **2006**, *128*, 7353–7359.
- [38] Á. Pekker, K. Kamarás, *Phys. Rev. B* **2011**, *84*, 075475.
- [39] S. A. Hodge, M. K. Bayazit, H. H. Tay, M. S. Shaffer, *Nat. Commun.* **2013**, *4*, 1989.
- [40] T. W. Odom, J. L. Huang, P. Kim, C. M. Lieber, *Nature* **1998**, *391*, 62–64.
- [41] L. H. Guan, Z. J. Shi, M. X. Li, Z. N. Gu, *Carbon* **2005**, *43*, 2780–2785.
- [42] C. Browne, S. Brenet, J. K. Clegg, J. R. Nitschke, *Angew. Chem. Int. Ed.* **2013**, *52*, 1944–1948; *Angew. Chem.* **2013**, *125*, 1998–2002.
- [43] A. M. Schimpf, K. E. Knowles, G. M. Carroll, D. R. Gamelin, *Acc. Chem. Res.* **2015**, *48*, 1929–1937.
- [44] E. L. Sceats, J. C. Green, *Phys. Rev. B* **2007**, *75*, 245441.
- [45] S. A. Hodge, H. H. Tay, D. B. Anthony, R. Menzel, D. J. Buckley, P. L. Cullen, N. T. Skipper, C. A. Howard, M. S. Shaffer, *Faraday Discuss.* **2014**, *172*, 311–325.

Received: May 4, 2016

Published online on July 28, 2016